BMB Reports - Manuscript Submission

Manuscript Draft

DOI: 10.5483/BMBRep.2022-0194

Manuscript Number: BMB-22-194

Title: Discovery of 14-3-3 zeta as a potential biomarker for cardiac hypertrophy

Article Type: Article

Keywords: 14-3-3 protein-zeta; cardiac hypertrophy induced cell; proteomic biomarker; acute myocardial infarction

Corresponding Author: Min-Jung Kang

Authors: Joyeta Mahmud[1,2,#], Hien Thi My Ong[1,2,#], Eda Ates[1,2], Hong Seog Seo[3], Min-Jung Kang[1,2,*]

Institution: [1]Center for Advanced Biomolecular Recognition, Korea Institute of Science and Technology,
[2]Division of Bio-Medical Science &Technology, KIST School, University of Science and Technology,
[3]Cardiovascular Center, Korea University Guro Hospital, Korea University Medicine,

Manuscript Type: Article

Discovery of 14-3-3 zeta as a potential biomarker for cardiac hypertrophy

Joyeta Mahmud[1, 2†], Hien Thi My Ong[1, 2†], Eda Ates[1, 2], Hong Seog Seo[3] and Min-Jung Kang[1, 2*]

[1]Center for Advanced Biomolecular Recognition, Korea Institute of Science and Technology, Seoul, 02792 Republic of Korea.

[2]Division of Bio-Medical Science & Technology, KIST School, University of Science and Technology, Seoul, 02792 Republic of Korea.

[3]Cardiovascular Center, Korea University Guro Hospital, Korea University Medicine, Seoul, 08308 Republic of Korea.

Running title: 14-3-3 protein-zeta in cardiac hypertrophy

† These authors contributed equally to this work

*** Corresponding author:**

Dr. Min-Jung Kang

Center for Advanced Biomolecular Recognition

Korea Institute of Science and Technology

Seoul, 02792, Republic of Korea

Tel: +82-2-958-5088

E-mail: mjkang1@kist.re.kr

ABSTRACT

Acute myocardial infarction (AMI) is a multifaceted syndrome influenced by the functions of various extrinsic and intrinsic pathways and pathological processes, which can be detected in circulation using biomarkers. In this study, we investigated the secretome protein profile of induced-hypertrophy cardiomyocytes to identify next-generation biomarkers for AMI diagnosis and management. Hypertrophy was successfully induced in immortalized human cardiomyocytes (T0445) by 200 nM ET-1 and 1 μM Ang II. The protein profiles of hypertrophied cardiomyocyte secretomes were analyzed by nano-liquid chromatography with tandem mass spectrometry and differentially expressed proteins that have been identified by Ingenuity Pathway Analysis. The levels of 32 proteins increased significantly (>1.4 fold), whereas 17 proteins (<0.5 fold) showed a rapid decrease in expression. Proteomic analysis showed significant upregulation of six 14-3-3 protein isoforms in hypertrophied cardiomyocytes compared to those in control cells. Multi-reaction monitoring results of human plasma samples showed that 14-3-3 protein-zeta levels were significantly elevated in patients with AMI compared to those of healthy controls. These findings elucidated the role of 14-3-3 protein-zeta in cardiac hypertrophy and cardiovascular disorders and demonstrated its potential as a novel biomarker and therapeutic strategy.

Keywords: 14-3-3 protein-zeta, cardiac hypertrophy induced cell, proteomic biomarker, acute myocardial infarction

INTRODUCTION

Cardiovascular diseases (CVDs) are a group of conditions that affect the heart and blood vessels, and they are the leading cause of death worldwide. According to the World Health Organization, CVDs account for over 17 million deaths each year, which is approximately 31% of all deaths worldwide (1). Hypertrophic cardiomyopathy (HCM) is a common genetic cardiac disease with a distribution of 1:200–1:500 in the general population (2). HCM is also associated with various severe symptoms including heart failure, valvular heart disease, arrhythmias, heart attack, and left ventricular hypertrophy. Diagnosing heart disorders is often difficult, and HCM is typically confirmed by cardiovascular imaging combined with echocardiography. However, diagnosis remains challenging for clinicians because of the diversity in disease manifestations along with differences in ventricular mass or morphologic expression across patients (3). The limited self-renewal capacity of myocardial cells complicates survival evaluation for patients with heart failure (4). Therefore, understanding the biological processes leading to cardiomyocyte hypertrophy and apoptosis is crucial for developing effective therapies (5). Proteomic studies have provided insights into the mechanisms underlying CVDs, especially in the development of biomarkers.

Current protein biomarkers for heart diseases include troponin I and T, myoglobin, creatine kinase, and creatine kinase-myoglobin (6). Natriuretic peptides are the most extensively studied but have not been used as biomarkers in clinical applications (7). Abnormal troponin expression is widely used as a diagnostic and prognostic marker for heart diseases. Troponin I and troponin T are highly sensitive in clinical samples, but their expression levels differ in patients with various heart syndromes.

Acute myocardial infarction (AMI), also known as a heart attack, is an obstruction condition that occurs when blood flow is abruptly disrupted, resulting in heart tissue or coronary artery injury (8). We have discovered obscurin and titin as biomarkers from human plasma using liquid chromatography with tandem mass spectrometry for AMI, which showed higher sensitivity than troponin I and T (9). Atrial natriuretic peptide (ANP) and brain natriuretic peptide (BNP), which have equivalent secretory profiles in cardiomyocyte under tension response, have been used as biomarkers to diagnose AMI and acute coronary syndrome in humans. However, the understanding of their biochemistry is limited, and post-translational modifications in their metabolism result in unsuccessful detection (10). In this study, we established an *in vitro* model of cardiac hypertrophy in a human cardiomyocyte line following angiotensin II (Ang II) and endothelin-1 (ET-1) treatment. Proteomic profiling of the secretome from the cell lines was performed using nano-LC-MS/MS, followed by the identification of high-abundance peptides. Candidate biomarkers were confirmed using a synthesized peptide using clinical samples. In this approach, we performed label-free quantitative analysis of potential biomarker candidates in human plasma of patients with AMI and healthy controls. Clinical biomarkers are generally discovered by analyzing clinical samples. Protein biomarkers that are differently expressed in serum samples of patients are compared with those of healthy controls. The biomarker candidates are then studied *in vitro* for their signaling pathways, cellular functions, and further networks. However, in this study, we attempted to discover biomarker candidates from a hypertrophy-induced cellular system using an *in silico* pathway analysis tool, and revealed useful biomarkers in clinical samples. Because the *in vitro* system does not reflect the volume of fluids in the human body, the secretome analysis results were inconsistent with those of the clinical sample analysis. Thus, analysis of the actual clinical sample is necessary to verify the significance of the excavated biomarker. Moreover, *in vitro* cellular systems have no limit on the number and amount of samples to be analyzed and is essential to study the effect of hypertrophic alterations on response to cellular mechanisms, protein expressions, and signaling pathway regulations. We first established the hypertrophy-induced human cardiac cellular system and then altered the proteomics process. Our study identified 14-3-3 protein-zeta as a potential biomarker for cardiac hypertrophy via proteome profiling and successfully validating clinical samples from patients with AMI. This study provides an outline for therapeutic targets of new biomarker strategies that enable the practice of related cardiac hypertrophy medicine.

RESULTS

In vitro cardiac hypertrophy model design

ET-1 and Ang II-treated immortalized human cardiomyocytes (T0445 cell line) were evaluated to determine their hypertrophic responses. The expression of sarcomeric α-actinin resulted in cytoskeletal actin rearrangement and increased cell surface area. Both hypertrophic reagents (11) showed a very similar increase in cell surface area after 4 h and 24 h of treatment, followed by the visible enlargement of actin fibrous tissue compared to untreated control cells (Fig. 1A). Moreover, the average cell surface areas of ET-1- and Ang II-treated cells were 3.5-fold higher than those of normal cells (Fig. 1B). Thus, cardiomyocyte hypertrophy was successfully induced by 200 nM ET-1 and 1 μM Ang II in T0445 cells. Immunocytochemistry revealed increased cell size and thickened cell membrane in the treated group compared to the control group. The phenotypical changes may include increased cell size, primary changes in the structures of the heart muscle cells, and alterations in the contractile properties of the heart. The significant change in cell size after treatment confirmed the induction of the disease model (Fig. 1A-B).

Western blots were performed to validate the successful induction of hypertrophy in the cardiomyocyte model; we confirmed the expression of secretome proteins at different time points over the treatment courses. The secretome of samples treated with 200 nM ET-1 showed significantly increased BNP expression after 15 min, 1 h, and 2 h, whereas ANP expression increased after 1, 2, 6, and 24 h of treatment (Figs 1C, 1D). In contrast, the 1 μM Ang II-treated secretome displayed a notable enhancement of BNP levels after 1, 2, 12, and 24 h, along with increased ANP expression after 15 min, 1 h, and 2 h of treatment (Figs 1E, 1F). BNP and ANP levels fluctuated according to time variations, and reproducibility increased 24 h after treatment.

Proteomic profiling of hypertrophic secretome

Proteomic analysis of hypertrophied and non-hypertrophied cardiomyocytes revealed distinct protein profiles. All total ion chromatogram data are shown in (Supplementary Figure 1), and the spectral count for all samples was 10 × E9.

A total of 200–300 proteins were identified from secretome proteins using Proteome Discoverer. Of these, 32 proteins with elevated levels were selected (Supplementary Table 1), showing the highest value of cross-correlation score (Xcorr) consistency for reproducibility in both ET-1 and Ang II treatment (fold change > 1.4). We identified several proteins that have already been proposed as cardiac hypertrophy biomarkers, such as talin-1 (12), filamin-A (13), follistatin-related protein 1 (14), profilin-1 (15,16), and vimentin (17,18). Our results showed the upregulation of six 14-3-3 protein isoforms (beta, epsilon, gamma, theta, zeta/delta, and eta) in both ET-1- and Ang II-treated cardiomyocytes.

The expression of 17 proteins was significantly downregulated in the secretome of hypertrophied cardiomyocytes in both treatments (ET-1 and Ang II) with reproducibility (Supplementary Table 2). Isoform 8 of filamin-B, alpha-2 HS-glycoprotein, glutathione S-transferase P, and T-complex protein 1 subunit beta and epsilon were reduced by 100-fold in hypertrophied cardiomyocytes compared to normal cells.

Canonical pathway analysis categorized the dramatically altered protein groups from ET-1- (Fig 2A) and Ang II-treated hypertrophied cardiomyocytes (Fig 2B). Among the most abundant signaling categories, 14-3-3-mediated signaling had the highest significance in both hypertrophied cardiomyocyte groups, whereas Hippo signaling was decreased. Protein–protein interaction networks analyzed by ingenuity pathway analysis (IPA) explored a tight and robust interaction network of the identified 14-3-3 family (Supplementary Figure 2A). Furthermore, our data revealed that 14-3-3 binding inactivates the Hippo signaling pathway by sequestering the YAP/TAZ function in the cytoplasm (Supplementary Figure 2B).

14-3-3 proteins as organ-specific biomarkers for cardiac hypertrophy

To verify the utility of 14-3-3 proteins as organ-specific biomarkers for cardiac hypertrophy, we analyzed the expression of six isoforms (Supplementary Table 3) from the secretome of different cell lines, including MKN-1 and HFE-145, Hep-3B and Hepa-RG, A549 and L132, and T0445, in control and hypertrophy treatment samples. In this context, we evaluated the relative intensity of the six 14-3-3 protein isoforms by ultra-high performance liquid chromatography–tandem mass spectrometry (UHPLC-MS/MS) coupled with multiple reaction monitoring (MRM). Peptide ions were selected for fragmentation using MS/MS, and spectrum MS/MS sequencing data are shown in Supplementary Figure 3.

The expression of 14-3-3 protein-gamma was extremely low, and was inconsistently detected in the samples. Therefore, we compared the intensity of five 14-3-3 isoforms between different cell lines including cardiomyocytes without hypertrophy induction by measuring the peak area ratios of one fragment ion from the internal standard (beta-actin) and the endogenous peptide. All five 14-3-3 protein isoforms were elevated in hypertrophy-induced cardiomyocytes, as revealed by MRM. The abundances of 14-3-3 protein-beta and protein-zeta/delta (Figs 3A,3C) showed the highest significant difference (>10-fold) intensity among all isoforms while 14-3-3 protein theta (Fig 3E) exhibited a lower expression (<2 fold) than other isoforms across cell lines. The expression of 14-3-3 protein-eta and protein-epsilon (Figs 3B,3D) were similar to those of different organ cells. The levels of 14-3-3 proteins were also measured in human plasma using ELISA (8 samples each from healthy controls and patients with AMI) and were elevated in all samples of patients with AMI compared to those of healthy controls (Supplementary Figure 4).

Validation of 14-3-3 protein-zeta in human plasma

Dual quantitative and qualitative analyses were used to confirm the biomarker candidates 14-3-3 protein-zeta/delta using synthesized peptide standards. 14-3-3 protein-zeta/delta was selected because its concentration in the secretome was significantly higher in induced cardiac hypertrophy cell lines than in other organ cell lines. The gradient and MS operating conditions and quantitative mass spectrometry with an MRM assay employed one unique peptide among the three transition ions monitored are presented in Supplementary Table 4. Representative MRM chromatograms obtained from 14-3-3 protein-zeta standard (Fig. 4A), T0445 control cell line (Fig. 4B), T0445 hypertrophied cell lines (Fig. 4C-D), and human plasma samples (Fig. 4E-F).

MRM assays were performed in 30 AMI and 23 healthy control plasma sample pools. The mass chromatogram peak areas from each run were calculated for 14-3-3 protein-zeta expression. The scatterplot distribution of the logarithm of average MRM peak areas (a.u.) according to the AMI/control status of the pool (Fig. 4G). Levels of 14-3-3 protein-zeta were found to be higher in the AMI group relative to those in the control group. Importantly, ROC curve analysis revealed AUC values of 0.854 (95% confidence interval (CI) 0.696–0.949) with a Youden index J of 0.6923, indicating the potential to use 14-3-3 protein-zeta expression as a biomarker for AMI diagnosis (Fig. 4H). These results demonstrated a strong correlation between spectral count–derived abundance and MRM peak area, indicating sensitivity and specificity of 69.2 and 100 respectively. Considering these findings, we identified a label-free quantitative analysis-based peptide that can differentiate between control and AMI groups with high specificity from logistic regression-based prediction modeling in clinical samples.

DISCUSSION

This study elucidated the role of the 14-3-3 protein family in HCM using nano-LC-MS/MS. Proteomic analysis revealed significant upregulation of 14-3-3 proteins in the secretome of the hypertrophy-induced heart cell line compared to the control. As shown in Tables 1 and 2, filamin B is a cytoplasmic actin-binding protein that has been found in human skeletal disorders and impaired microvascular environments (19). T-complex protein 1 is a chaperonin that plays an important role in the folding of cytoskeletal proteins (20). Histone 1.5 is a linker protein that binds and affects chromatin (21). Histone 1.3 elevation has been reported as a prognostic biomarker for pancreatic ductal adenocarcinoma (22). Histone proteins appear to be downregulated by anti-apoptotic cell reactions. As shown in Table 2, gelsolin, alpha-2-macroglobulin, and elongation factor 1-alpha 1 were downregulated. Gelsolin is an actin-binding protein known for its role in cell motility and apoptosis (23).

Considering the complex underlying pathogenic factors associated with cardiomyocyte hypertrophy, we investigated the secretome to identify proteins related to this condition. The study of secretome, which consists of extracellular proteins, has gained significant attention in the research community owing to their potential to reveal biomarkers and new therapeutic targets (24). The 14-3-3 isoform proteins are expressed in high levels in the brain, skeletal muscles, heart, and embryonic stem cells with a wide range of roles in cell signaling. After platelet activation, 14-3-3 protein-zeta was localized in and secreted from dense granules (25). Transport vesicles budding from the endoplasmic reticulum carry these secreted proteins from the inside of the cell to the cell surface. From there, the vesicles fuse with the plasma membrane, releasing 14-3-3 protein into the extracellular space (26).

14-3-3 protein-zeta constrains the insulin secretion in patients with type 2 diabetes by regulating mitochondrial function. Mice that expressed dominant-negative 14-3-3 mutant protein in the myocardium showed increased occurrence of cardiac hypertrophy, fibrosis, and inflammation after diabetes induction (27). Thus, modulating 14-3-3 protein expression may serve as a novel therapeutic approach against diabetes-associated cardiovascular complications. However, the exact underlying mechanism is not fully elucidated due to its diverse structure and protein interaction. Further studies are required to assess the functional role of 14-3-3 protein-zeta in cardiac hypertrophy.

This study showed that several signaling pathways were activated or inhibited in response to HCM. The IPA results revealed that the most activated upstream regulators were glycolysis, actin cytoskeletal signaling, and 14-3-3 mediated signaling. In contrast, the most inhibited regulator was the Hippo signaling pathway, with a z-score <-2. The Hippo signaling pathway controls organ size by suppressing cell proliferation, limiting cell size, and inducing apoptosis. The inactivation of this pathway or activation of its downstream effectors has been reported to improve cardiac regeneration (28,29). Studies have also established the crucial role of the actin cytoskeleton in regulating the Hippo-YAP/TAZ signaling pathway (30).

Consistent with the proteomic analysis data obtained from the cardiomyocyte secretome, 14-3-3 protein-zeta was significantly upregulated in the hypertrophy model. Therefore, we further performed an *in vivo* label-free quantitative analysis of plasma from patients with AMI and healthy control samples. Blood plasma circulates through the whole body, and therefore, it contains large extracellular vesicles such as proteins, lipids, and nucleic acids, which are often key biomarkers in clinical samples. We explored the potential functional roles of 14-3-3 protein–protein interactions in the heart as a target therapeutic strategy. We further suggest that the interactomes of 14-3-3 protein-zeta in hypertrophy-induced cardiac cells should be explored. The 14-3-3 protein network regulates cardiac ATP production via interactions with inner membrane proteins and metabolizes fatty acid via enzymes within the mitochondrial matrix. Therefore, the interactomes of cardiac 14-3-3 could be potentially therapeutic in the proteostasis of cardiovascular metabolic disease. The increased levels of 14-3-3 protein-zeta *in vitro* and in patients with AMI could suggest that 14-3-3 protein-zeta plays a role in the development of cardiac hypertrophy and represents a therapeutic target for treatment. 14-3-3 protein-zeta could be targeted by developing drugs that specifically inhibit its function or prevent its interaction with other proteins involved in the development of cardiac hypertrophy. Furthermore, RNA interference could be used to reduce the expression of 14-3-3 protein-zeta, decreasing its contribution to cardiac hypertrophy.

MATERIALS AND METHODS

Cell culture and *in vitro* hypertrophy model

The immortalized human cardiomyocyte cell line T0445 was obtained from Applied Biological Materials Inc. (Abm, Richmond, BC, Canada). The human normal lung epithelial cell line (L132), human lung cancer cell line (A549), human gastric cancer cell line (MKN-1), human normal gastric cell line (HFE-145), and human liver cancer cell line (Hep3B) were obtained from the Korea Cell Line Bank (KCLB, Seoul, South Korea). The human normal liver cell line (Hepa RG) was obtained from Thermo Fisher Scientific (Massachusetts, USA). All cell lines were regularly cultured in RPMI, DMEM, Williams medium E media (Gibco, USA), and Prigrow I media (ABM, Richmond, BC, Canada) supplemented with 10% heat-inactivated fetal bovine serum (Gibco, USA) and 1% penicillin–streptomycin (Gibco, USA). Culture plates were maintained at 37°C with 5% CO_2 in a humidified cell incubator.

Hypertrophic agonists ET-1 and Ang II were purchased from Sigma-Aldrich (Darmstadt, Germany). Cardiomyocytes were treated with 1 μM Ang II and 200 nM ET-1 (Sigma-Aldrich, Darmstadt, Germany) diluted in an appropriate medium.

LC-MS/MS analysis

LTQ-Orbitrap Velos Pro combined with the EASY-nLC1000 system (ThermoFisher Scientific, USA) was used for proteomic profiling. Peptide separation was achieved using an Acclaim PepMap EASY-Spray analytical column (75 μm × 50 cm, nanoViper, 100 Å, C18, 2 μm) (Thermo Scientific, USA). The CM and human plasma samples were tested using a UHPLC-MS/MS system connected to an LTQ Orbitrap Velos Pro and separated using a 4 μm Proteo Phenomenex (90 Å pore, LC Column 250 × 4.6 mm) (Jupiter, USA). The spray voltage was

+3.9 kV, and the eluted peptides were examined. MRM was used to quantitatively analyze six 14-3-3 protein isotypes and beta-actin simultaneously.

Protein identification and ingenuity pathway analysis

The MS/MS data obtained from sample analysis were searched using the Proteome Discoverer v2.2 (ThermoFisher Scientific, USA) search engine against the SEQUEST algorithm with amino acid sequences in the SwissProt database (2017). The results were searched using the Percolator for scoring. The followed database parameters were applied: trypsin digestion of the enzyme, fragment ion mass tolerance of 0.6 Da, precursor ion mass tolerance of 10 ppm, allowance of a maximum of 2 missed cleavages, and carbamidomethyl and oxidation as variable modifications with respective masses of +57.021 Da and +15.995 Da. The peptide matching criteria were set as a SEQUEST HT score of >1, and Xcorr criteria of >1.2 for (+1) peptides, >1.9 for (+2) peptides, and >2.3 for (+3) peptides. A unique peptide number of at least 2 per protein was required to ensure reliability. Differences between the two groups were considered statistically significant at $p < 0.05$.

All identified differentially expressed proteins in hypertrophied and non-hypertrophied cardiomyocytes were subjected to protein pathway analysis using IPA tools (http://www.ingenuity.com) (Qiagen, Germany). The z-score value (> 2.0) was predicted as the activation state of canonical pathways, whilst the inhibition state was defined by z-score < −2.0.

Supplementary methods

Western blot, ELISA, immunocytochemistry analysis, sample preparation, in-solution trypsin digestion, data availability, and data processing are described in the supplementary information.

Acknowledgments

This study was supported by the National Research Foundation of Korea (NRF) and funded by the Ministry of Science and ICT, Republic of Korea (no. NRF-2017R1A2B2004398, NRF-2021R1A2C209370611), and the Korea Institute of Science and Technology (KIST) Institutional Program (2E31623).

Ethical approval

The Institutional Review Board of the Korea University Medical Center approved the sample collection and analysis (KUGH12118-005).

Conflicts of interest

The authors have no conflicting interests.

FIGURE LEGENDS

Figure 1. Immunocytochemistry and western blot analysis of BNP and ANP expressions in T0445 cells treated with 200 nM ET-1 and 1 μM Ang II

(A) Immunostaining results show α-actinin (green) and nucleus (blue)

(B) Bar chart showing relative signal intensity on average cell surface area

(C) Western blotting of ET-1-treated secretome

(D) Relative expression changes of ET-1-treated secretome

(E) Western blotting of Ang II-treated secretome

(F) Relative expression changes of Ang II-treated secretome

Figure 2. Identification of differentially expressed proteins in canonical pathways identified using Ingenuity Pathway Analysis of treated secretome

(A) ET-1-treated secretome

(B) Ang II-treated secretome

Bar charts representing fold-change in protein intensity between the treated group and untreated T0445 cells. Columns represent canonical pathways.

Figure 3. Relative intensity of 14-3-3 protein isoforms in the secretome of hypertrophied cardio myocytes together with different organ cells

(A) 14-3-3 protein-beta

(B) 14-3-3 protein-theta

(C) 14-3-3 protein-zeta/delta

(D) 14-3-3 protein-epsilon

(E) 14-3-3 protein-etha

Figure 4. Representative selected reaction monitoring chromatograms and performance in human plasma samples of 14-3-3 protein-zeta

(A) 14-3-3 protein-zeta standard

(B) T0445 secretome

(C) ET-1- treated T0445 secretome

(D) Ang-II-treated T0445 secretome

(E) Healthy control human plasma

(F) AMI human plasma

(G) Box-and-whiskers plot showing the levels of 14-3-3 protein-zeta in healthy controls (n = 23) and patients with AMI (n = 30)

(H) ROC analysis distinguishing the diagnostic accuracy of 14-3-3 protein-zeta expression between patients with AMI and healthy controls.

REFERENCES

1. Thrift AG, Thayabaranathan T, Howard G, *et al* (2017) Global stroke statistics. Int J Stroke 12, 13-32
2. Maron BJ (2018) Clinical course and management of hypertrophic cardiomyopathy. NJEM 379, 655-668
3. Rowin EJ, Maron BJ, Maron MS (2020) The hypertrophic cardiomyopathy phenotype viewed through the prism of multimodality imaging: clinical and etiologic implications. Cardiovasc Imag 13, 2002-2016
4. Laflamme MA and Murry CE (2011) Heart regeneration. Nature 473, 326-335
5. Babuin L, Jaffe AS (2005) Troponin: the biomarker of choice for the detection of cardiac injury. CMAJ 173, 1191-1202
6. Garg P, Morris P, Fazlanie AL, et al (2017) Cardiac biomarkers of acute coronary syndrome: from history to high-sensitivity cardiac troponin. Intern Emerg Med 12, 147-155
7. Mueller T, Gegenhuber A, Poelz W, Haltmayer M (2005) Diagnostic accuracy of B type natriuretic peptide and amino terminal proBNP in the emergency diagnosis of heart failure. Heart 91, 606-612
8. Toldo S and Abbate A (2018) The NLRP3 inflammasome in acute myocardial infarction. Nat Rev Cardiol 15, 203-214
9. Kang MJ, Seong Y, Mahmud J, Nguyen BT (2020) Obscurin and clusterin elevation in serum of acute myocardial infarction patients. Bull Korean Chem Soc 41, 266-273
10. Chan D, Ng LL (2010) Biomarkers in acute myocardial infarction. BMC Med 8, 1-11

11. Watkins SJ, Borthwick GM, Arthur HM (2011) The H9C2 cell line and primary neonatal cardio myocyte cells show similar hypertrophic responses in vitro. In Vitro Cell Dev Biol Anim 47, 125-131

12. Manso AM, Li R, Monkley SJ, et al (2013) Talin1 has unique expression versus talin 2 in the heart and modifies the hypertrophic response to pressure overload. J Biol Chem 288, 4252-4264

13. Bandaru S, Ala C, Zhou AX, Akyürek LM (2021) Filamin A regulates cardiovascular remodeling. Int J Mol Sci 22, 6555

14. Lee SY, Kim DY, Kyung Kwak M, et al (2019) High circulating follistatin-like protein 1 as a biomarker of a metabolically unhealthy state. Endocr J 66, 241-251

15. Paszek E, Żmudka K, Plens K, Legutko J, Rajs T, Zajdel W (2020) Evaluation of profilin 1 as a biomarker in myocardial infarction. Eur Rev Med Pharmacol Sci 24, 8112-8116

16. Yang D, Wang Y, Jiang M, et al (2017) Downregulation of profilin-1 expression attenuates cardiomyocytes hypertrophy and apoptosis induced by advanced glycation end products in H9c2 cells. Biomed Res Int 2017, 9716087

17. Klopsch C, Gaebel R, Lemcke H, et al (2018) Vimentin-induced cardiac mesenchymal stem cells proliferate in the acute ischemic myocardium. Cells Tissues Organs 206, 35-45

18. Gong DH, Dai Y, Chen S, et al (2019) Secretory vimentin is associated with coronary artery disease in patients and induces atherogenesis in ApoE(-/-) mice. Int J Cardiol 283, 9-16

19. Zhou X, Tian F, Sandzén J, et al (2007) Filamin B deficiency in mice results in skeletal malformations and impaired microvascular development. Proc Natl Acad Sci USA 104, 3919-3924
20. Carrascosa JL, Llorca O, Valpuesta JM (2001) Structural comparison of prokaryotic and eukaryotic chaperonins. Micron 32, 43-50
21. Li JY, Patterson M, Mikkola HK, Lowry WE, Kurdistani SK (2012) Dynamic distribution of linker histone H1.5 in cellular differentiation. PLoS Genet 8, e1002879
22. Bauden M, Kristl T, Sasor A, et al (2017) Histone profiling reveals the H1.3 histone variant as a prognostic biomarker for pancreatic ductal adenocarcinoma. BMC Cancer 17, 810
23. Silacci P, Mazzolai L, Gauci C, Stergiopulos N, Yin HL, Hayoz D (2004) Gelsolin superfamily proteins: key regulators of cellular functions. Cell Mol Life Sci 61, 2614-2623
24. Severino V, Farina A, Chambery A (2013) Analysis of secreted proteins. Methods Mol Biol 1002, 37-60
25. Hernandez-Ruiz L, Valverde F, Jimenez-Nuñez MD, et al (2007) Organellar proteomics of human platelet dense granules reveals that 14-3-3ζ is a granule protein related to atherosclerosis. J Proteome Res 6, 4449-4457
26. Thompson WC and Goldspink PH (2022) 14–3-3 protein regulation of excitation–contraction coupling. Pflug Arch Eur J Phy 1-13
27. Mugabo Y, Zhao C, Tan JJ, et al (2022) 14-3-3ζ Constrains insulin secretion by regulating mitochondrial function in pancreatic β cells. JCI insight, 7

28. Zhou Q, Li L, Zhao B, Guan K (2015) The hippo pathway in heart development, regeneration, and diseases. Circ Res 116, 1431-1447

29. Zhou W and Zhao M (2018) How hippo signaling pathway modulates cardiovascular development and diseases. J Immuno Res, 2018

30. Seo J and Kim J (2018) Regulation of hippo signaling by actin remodeling. BMB Rep 51, 151-156

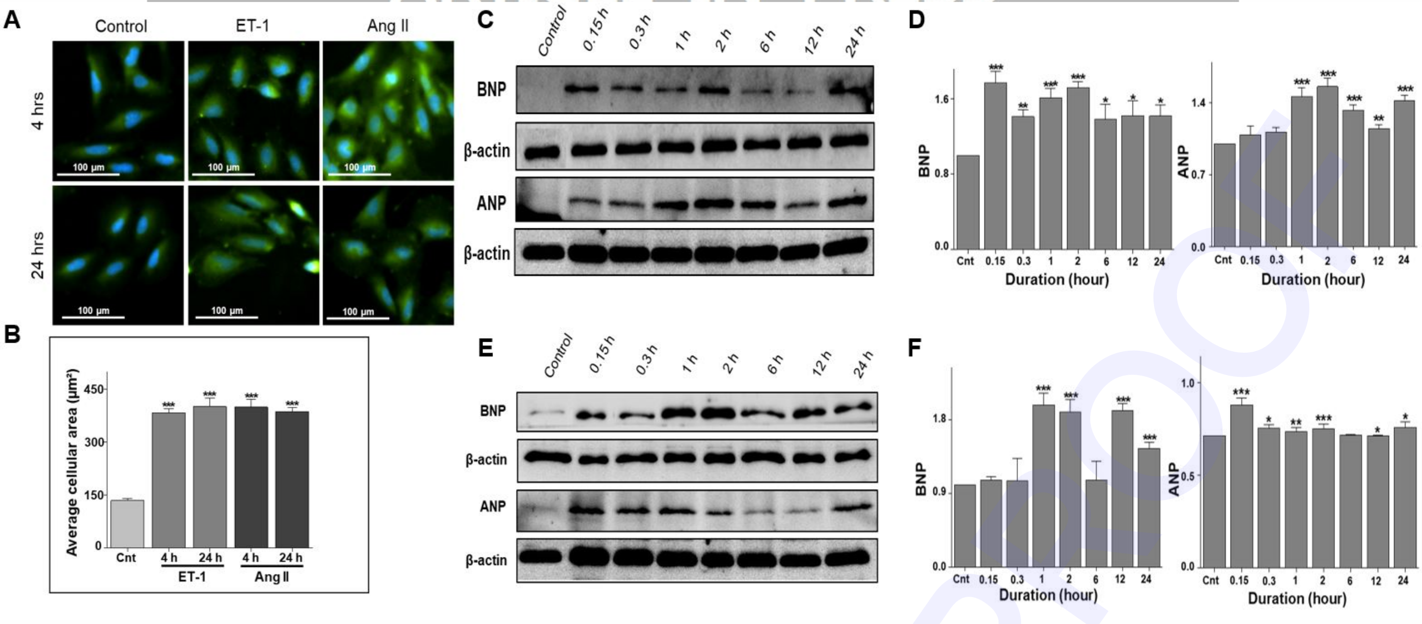
A
Control
ET-1
Ang II
4 hrs
24 hrs
100 µm
B
Average cellular area (µm²)
Cnt
4 h
24 h
ET-1
Ang II
C
Control
0.15 h
0.3 h
1 h
2 h
6 h
12 h
24 h
BNP
β-actin
ANP
D
Duration (hour)
E
F

Fig. 1.

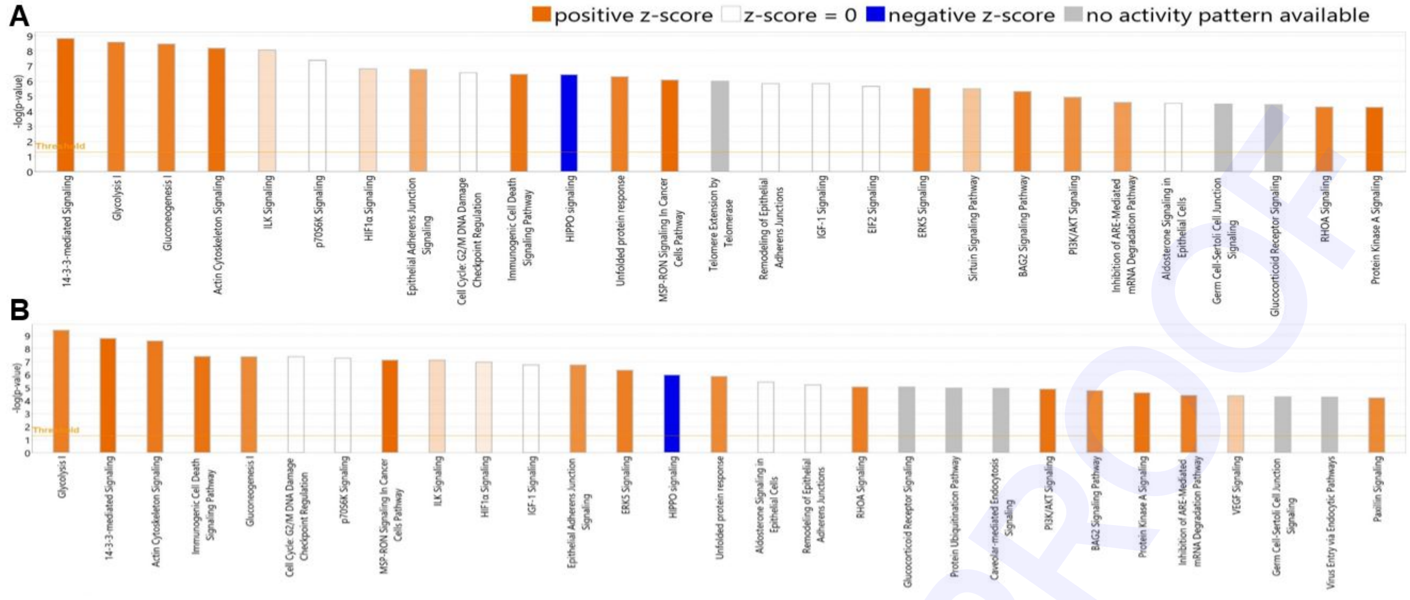
A
positive z-score
z-score = 0
negative z-score
no activity pattern available
-log(p-value)
Threshold
14-3-3-mediated Signaling
Glycolysis I
Gluconeogenesis I
Actin Cytoskeleton Signaling
ILK Signaling
p70S6K Signaling
HIF1α Signaling
Epithelial Adherens Junction Signaling
Cell Cycle: G2/M DNA Damage Checkpoint Regulation
Immunogenic Cell Death Signaling Pathway
HIPPO signaling
Unfolded protein response
MSP-RON Signaling In Cancer Cells Pathway
Telomere Extension by Telomerase
Remodeling of Epithelial Adherens Junctions
IGF-1 Signaling
EIF2 Signaling
ERK5 Signaling
Sirtuin Signaling Pathway
BAG2 Signaling Pathway
PI3K/AKT Signaling
Inhibition of ARE-Mediated mRNA Degradation Pathway
Aldosterone Signaling in Epithelial Cells
Germ Cell-Sertoli Cell Junction Signaling
Glucocorticoid Receptor Signaling
RHOA Signaling
Protein Kinase A Signaling
B
-log(p-value)
Threshold
Glycolysis I
14-3-3-mediated Signaling
Actin Cytoskeleton Signaling
Immunogenic Cell Death Signaling Pathway
Gluconeogenesis I
Cell Cycle: G2/M DNA Damage Checkpoint Regulation
p70S6K Signaling
MSP-RON Signaling In Cancer Cells Pathway
ILK Signaling
HIF1α Signaling
IGF-1 Signaling
Epithelial Adherens Junction Signaling
ERK5 Signaling
HIPPO signaling
Unfolded protein response
Aldosterone Signaling in Epithelial Cells
Remodeling of Epithelial Adherens Junctions
RHOA Signaling
Glucocorticoid Receptor Signaling
Protein Ubiquitination Pathway
Caveolar-mediated Endocytosis Signaling
PI3K/AKT Signaling
BAG2 Signaling Pathway
Protein Kinase A Signaling
Inhibition of ARE-Mediated mRNA Degradation Pathway
VEGF Signaling
Germ Cell-Sertoli Cell Junction Signaling
Virus Entry via Endocytic Pathways
Paxillin Signaling

Fig. 2.

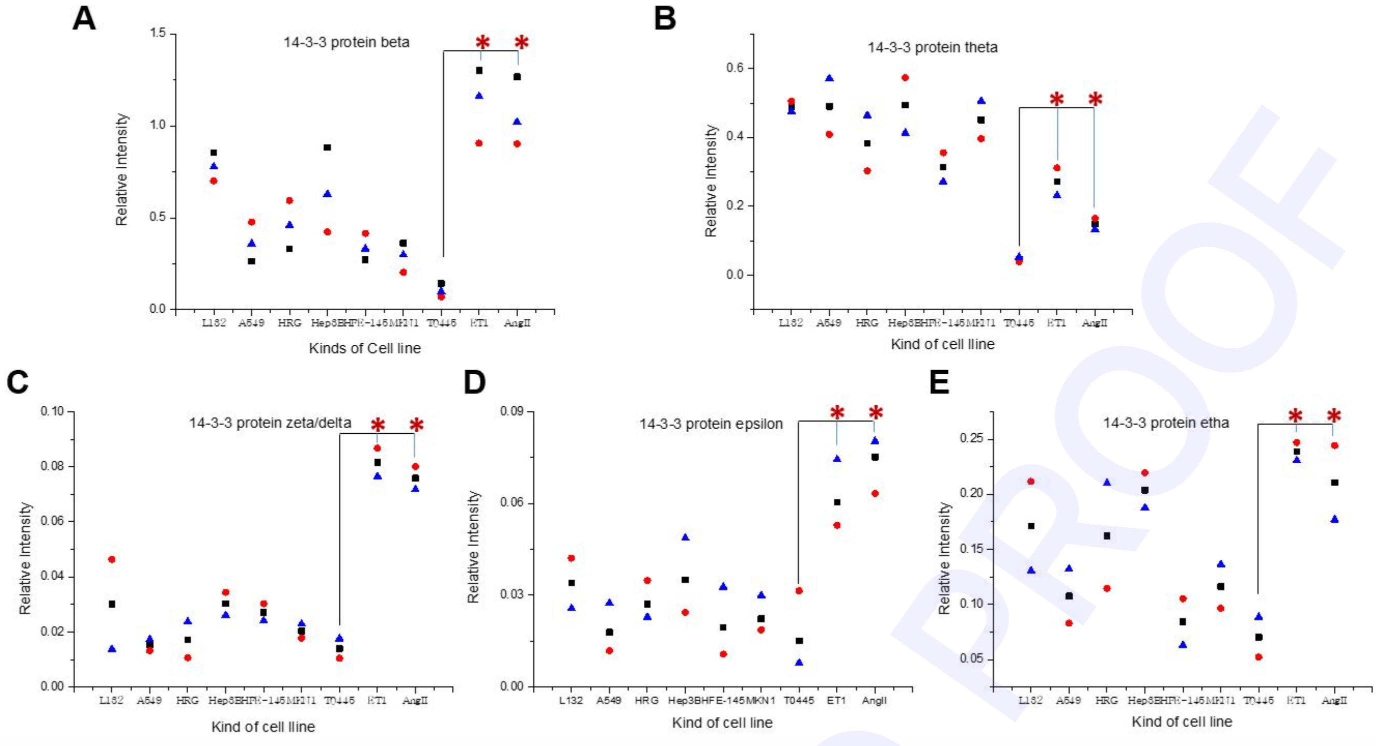
A
14-3-3 protein beta
Relative Intensity
Kinds of Cell line
L132 A549 HRG Hep3B HFE-145 MKN1 T0445 ET1 AngII
B
14-3-3 protein theta
Relative Intensity
Kind of cell lline
C
14-3-3 protein zeta/delta
Relative Intensity
Kind of cell lline
D
14-3-3 protein epsilon
Relative Intensity
Kind of cell line
E
14-3-3 protein etha
Relative Intensity
Kind of cell line

Fig. 3.

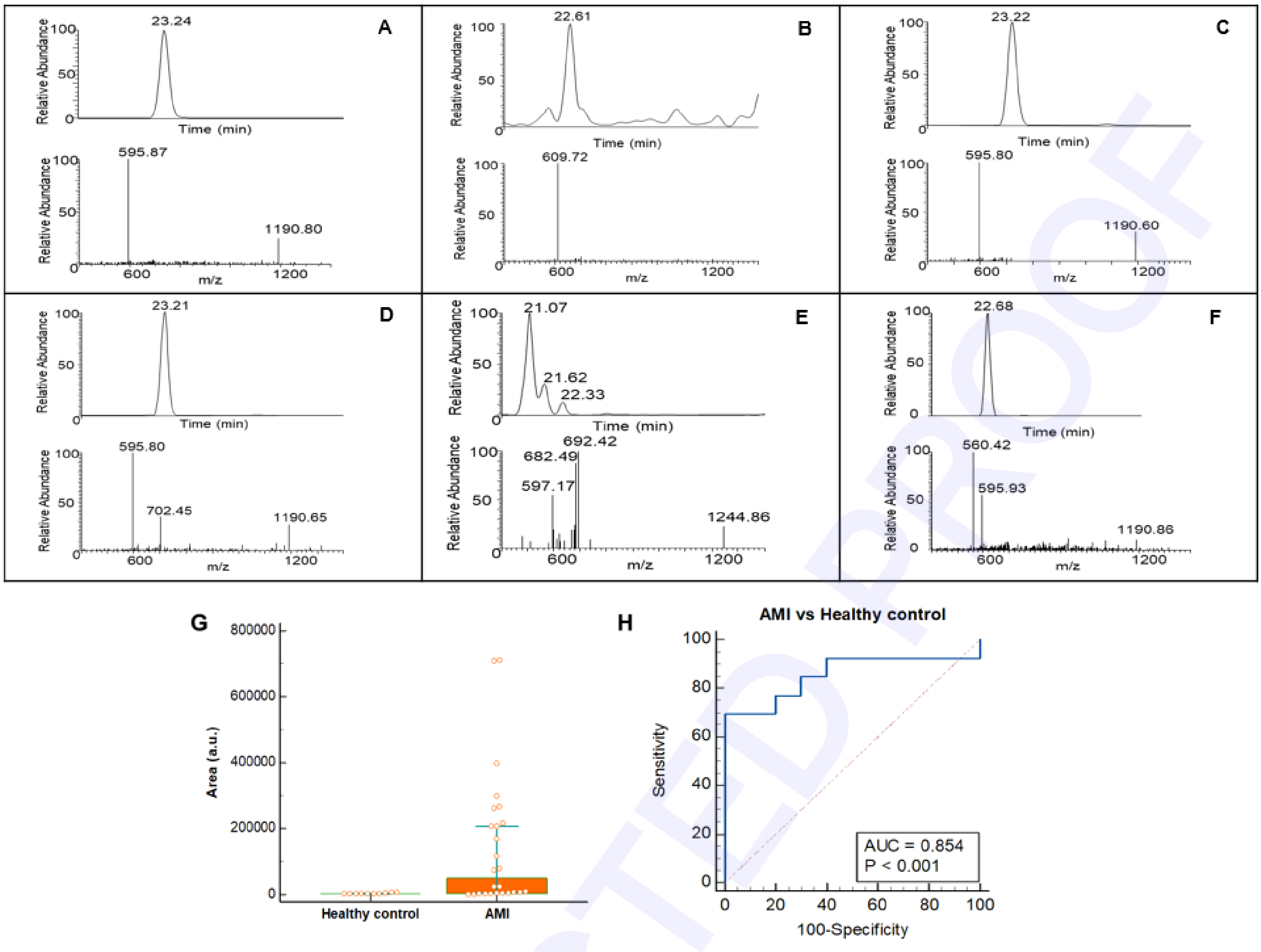
A
B
C
D
E
F
G
H
Relative Abundance
Time (min)
m/z
23.24
595.87
1190.80
22.61
609.72
23.22
595.80
1190.60
23.21
595.80
702.45
1190.65
21.07
21.62
22.33
692.42
682.49
597.17
1244.86
22.68
560.42
595.93
1190.86
Area (a.u.)
Healthy control
AMI
AMI vs Healthy control
Sensitivity
100-Specificity
AUC = 0.854
P < 0.001

Fig. 4.

Abbreviations

AMI	Acute myocardial infarction
Ang II	Angiotensin II
ANP	Atrial natriuretic peptide
Ask-1	Apoptosis signal-regulating kinase 1
BAD	Bcl-2-associated death promoter
BCA	Bicinchoninic acid assay
BNP	Brain natriuretic peptide
CM	Conditioned media
ET-1	Endothelin-1
ELISA	Enzyme-linked immunosorbent assay
FBS	Fetal Bovine Serum
TBS	Tris-Buffered Saline
TIC	Total ion chromatogram
IPA	Ingenuity pathway analysis
JNK	c-Jun N-terminal kinase
MAPK	Mitogen-activated protein kinase
LC-MS/MS	Liquid Chromatography with tandem mass spectrometry
UHPLC	Ultra-high performance liquid chromatography

Supplementary methods, figures and tables for:

Discovery of 14-3-3 zeta as a potential biomarker for cardiac hypertrophy

Joyeta Mahmud[1, 2†], Hien Thi My Ong[1, 2†], Eda Ates[1, 2], Hong Seog Seo[3] and Min-Jung Kang[1, 2*]

[1]Center for Advanced Biomolecular Recognition, Korea Institute of Science and Technology, Seoul, 02792 Republic of Korea.

[2]Division of Bio-Medical Science & Technology, KIST School, University of Science and Technology, Seoul, 02792 Republic of Korea.

[3]Cardiovascular Center, Korea University Guro Hospital, Korea University Medicine, Seoul, 08308 Republic of Korea.

Running title: 14-3-3 protein-zeta in cardiac hypertrophy

† These authors contributed equally to this work

*** Corresponding author:**

Dr. Min-Jung Kang

Center for Advanced Biomolecular Recognition

Korea Institute of Science and Technology

Seoul, 02792, Republic of Korea

Tel: +82-2-958-5088

E-mail: mjkang1@kist.re.kr

Supplementary Methods

Western blot, ELISA, and immunocytochemistry

A total of 30 μg of protein from each sample was separated by one-dimensional 12% Tris-glycine SDS-PAGE then transferred to nitrocellulose membranes (Bio-Rad, CA, USA). TBST containing 5% skim milk was used for blocking the membrane for 1 h followed by washing three times with TBST. Nitrocellulose membranes were incubated overnight with the primary antibodies at 1:1000 in 5% BSA at 4 ℃ in the dark, and 1:5000 horseradish peroxidase-conjugated secondary antibodies (Cell Signaling Technology, Massachusetts, USA) were added to 5% skim milk. The membranes were incubated at room temperature for 1 h. Blots were detected using a chemiluminescence reagent (Santa Cruz Biotechnology, Massachusetts, USA) by the Ez-Capture MG system (ATTO, NY, USA), and the relative intensity of the western blot bands was measured using ImageJ 1.53a (National Institutes of Health, USA). Anti-β-actin antibody was purchased from Cell Signaling Technology (Massachusetts, USA) and used as a loading control. The anti-ANP and anti-BNP antibodies used in this study were purchased from Thermo Fisher Scientific (Massachusetts, USA).

Human plasma samples were analyzed using a commercial ELISA kit MBS269690 (MyBioSource Inc., CA, USA) according to the manufacturer's instructions. An automated microplate reader (Bio-Rad, Hercules, CA, USA) was used to measure optical density at 450 nm. The concentration of each sample was determined based on absorbance and normalized to the standard.

The cells were seeded onto glass coverslips for immunocytochemistry analysis and incubated with hypertrophic agonists. To fix samples, 4% formaldehyde (Sigma, USA) was used for 20 min, and immunofluorescence staining was performed. Triton (2%) and Triton X-100 (0.1%) were used for blocking nonspecific binding for 30 min. After, cells were incubated with anti-sarcomeric alpha-actinin (Abcam, USA) and kept at 4 °C overnight. The secondary antibody Alexa Fluor 488 goat anti-mouse IgG (H+L) (Thermo Fisher Scientific, USA) was used for incubation for 2 h at room temperature. Nuclei were stained with Hoechst 33342 (Thermo Fisher Scientific, USA), coverslips were mounted with mounting solution, and images were obtained using a Nikon inverted microscope Eclipse Ti-U (Carl Zeiss, Germany). ImageJ 1.53a (National Institutes of Health, USA) was used to measure the cell area (unit: μm^2).

Sample preparation

The culture medium was replaced with serum-free medium for 24 h. The conditioned medium (CM) was collected and centrifuged at 10,000×g for 15 min at 4 °C to remove cell debris. The collected supernatant was transferred into a new tube, and the protein concentration was measured and freeze-dried using an ALPHA 1-2 LDPlus instrument (Martin Christ Gefriertrocknungsanlagen Gmb, Osterode am Harz, Germany). HFE-145, MKN-1, L132, A549, Hep3B, Hepa RG, T0445, ET-1, and Ang II-induced T0445 cell lysates were collected after washing with cold PBS twice. TNN-EDTA lysis buffer (Thermo Scientific, Massachusetts USA) with protease and phosphatase inhibitor cocktail (Roche Diagnostics GmbH, Mannheim, Germany) was added after cells were collected. Cell lysates were incubated at 4 °C for 30 min and vortexed twice after 10 min periods. The samples were centrifuged for 15 min at 10,000×g and 4 °C for supernatant collection. Finally, a BCA kit (Thermo Scientific, Massachusetts, USA) was used to measure protein concentrations according to the manufacturer's instructions.

Plasma samples were collected from AMI patients (n=30) and healthy controls (n=23) in 2013. The control group was subjected who did not have any historical record of cardiovascular disease or acute renal and hepatic diseases. Written informed consent was obtained from all participants at the Korea University Medical Center (Seoul, Korea). The collected blood was centrifuged for 40 min at 10,000 × g at 4 °C, followed by the addition of 0.6 TIU/mL aprotinin and storage at -70 °C until testing. Plasma samples were digested in solution and quantitatively analyzed by ELISA and UHPLC-MS/MS using MRM.

In-solution trypsin digestion

After measuring the concentration of each sample, 200 µg of the cell lysate was dried in a speed vacuum dryer for 3 h. The dried samples were reconstituted with 6.0 M urea (Sigma, USA) and reduced by incubation in 200 mM dithiothreitol (DTT; Sigma-Aldrich, Darmstadt, Germany) for 30 min at 37 °C. Then, samples were alkylated in 100 mM iodoacetamide (IAA; Sigma-Aldrich, Darmstadt, Germany) for 30 min at 37 °C. Trypsin (Sigma-Aldrich, Darmstadt, Germany) was added to samples at a final protease: protein ratio of 1:30 (w/w), and the mixture was incubated at 37 °C for 20 h. The samples were then cleaned using a C18 spin column according to the manufacturer's instructions (Pierce, Thermo Fisher Scientific, USA). After cleaning, samples were dried using a vacuum freeze dryer and reconstituted in 0.1% formic acid (Thermo Scientific, Spain).

The CM sample and human plasma were reconstituted with 8.0 M urea (Sigma, USA), reduced by incubation in 100 mM DTT (Sigma-Aldrich, Darmstadt, Germany) for 30 min at 37 °C and alkylated in 500 mM IAA (Sigma-Aldrich, Darmstadt, Germany) for 30 min at 37 °C in the dark. Trypsin (Sigma-Aldrich, Darmstadt, Germany) was added to the sample at a final protease: protein ratio of 1:30 (w/w), and the mixture was incubated at 37 °C for 20 h.

Carbamidomethyl modification (+57.07 Da) of the standard peptide was performed using an iodoacetamide alkylating reagent (Thermo Fisher Scientific, Massachusetts, USA). According to manufacturer's protocol, 10 µl of 2% SDS and 90 µl of 200 mM ammonium bicarbonate (pH 8.0) were added to 200 µg of peptide sample, then ultrapure water was adjusted to a volume of 200 µl. Ten µl of 200 mM Tris(2-carboxyethyl) phosphine hydrochloride was added and incubated at 55°C for 1 hour. The sample was alkylated for 30 minutes by 10 µl of 375 mM iodoacetamide protected from light.

All samples were desalted using a peptide desalting spin column, according to the manufacturer's instructions (Thermo Fisher Scientific, Massachusetts, USA). After the vacuum freeze-drying process, samples were reconstituted with 0.1% formic acid (Thermo Scientific, Spain).

Data availability

The mass spectrometry proteomics data have been deposited to the public and global open access database "PRIDE" in ProteomeXchange consortium (http://www.proteomexchange.org) with the database identifier PXD020701.

Data Processing

All data are presented as mean ± standard deviation (SD), and analyses were conducted in triplicate. The western blot results were reported as fold change compared to β-actin and control. Differences between the two groups were determined by a Student's t-test (Origin 2017, USA). The significance of data was accepted when p value was lower than 0.05 (*$P \leq 0.05$, **$P \leq 0.01$, and ***$P \leq 0.005$). The MedCalc Statistical Software version 19.2.6 (https://www.medcalc.org; 2020) (Ostend, Belgium) was used to perform ROCs and to calculate AUCs and other comparisons (i.e. sensitivity, specificity, and accuracy).

Supplementary Figure 1. Total ion chromatogram of human cardiomyocytes (T0445) secretome

(A) Control

(B) Ang II treated

(C) ET-1 treated.

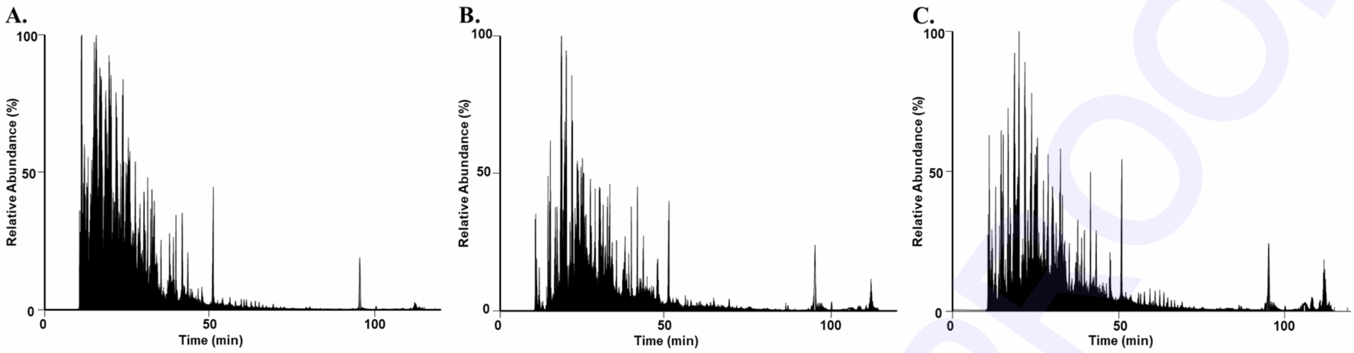

Supplementary Figure 2. Analysis of differentially expressed protein regulatory pathways in control and hypertrophy induce secretome.

(A) 14-3-3 mediated signaling

(B) Hippo signaling

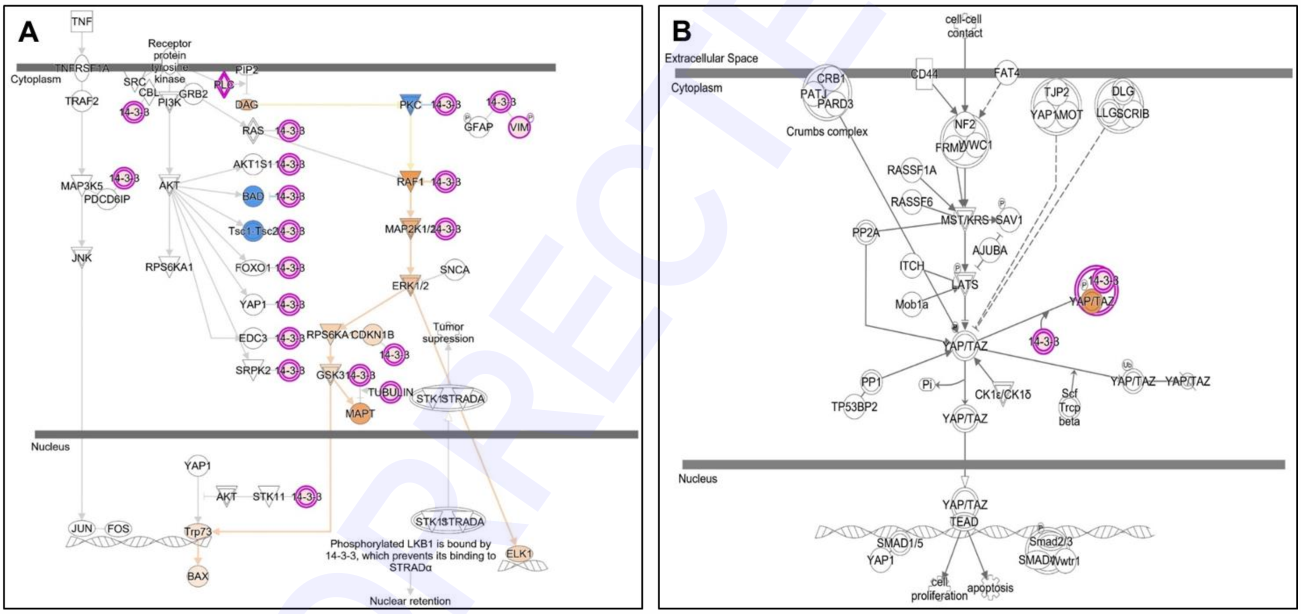

Supplementary Figure 3. The representative MS/MS spectrum of six isoforms from14-3-3 protein

(A)14-3-3 beta, m/z 720.7

(B) 14-3-3 epsilon, m/z 739

(C) 14-3-3 gamma, m/z 711

(D) 14-3-3 theta, m/z 696.4

(E) 14-3-3 zeta/delta, m/z 710

(F) 14-3-3 eta, m/z 874

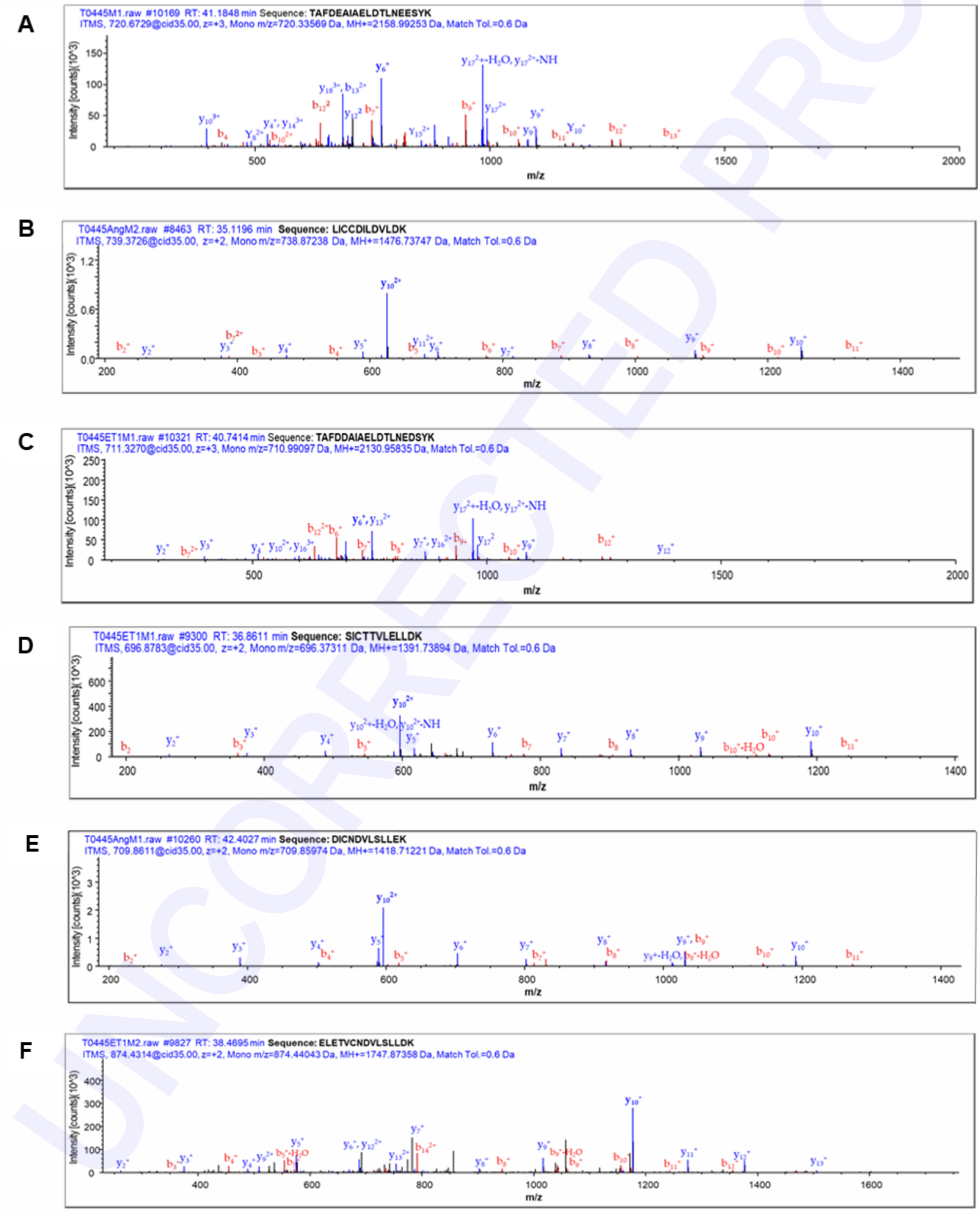

Supplementary Figure 4. Measured levels of 14-3-3 protein in human plasma AMI and healthy control.

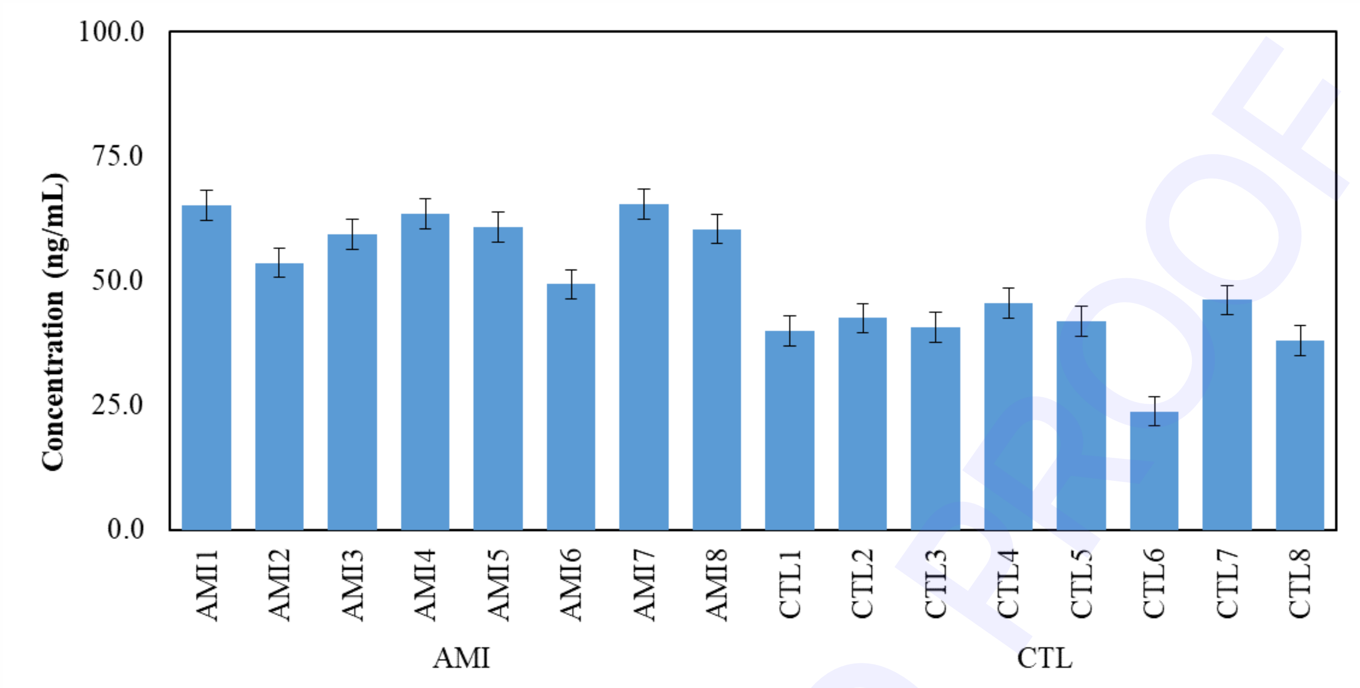

Supplementary Table 1. Proteomic profiling by nanoLC-MS/MS. 32 proteins were upregulated in both treated (ET-1 and Ang II) cardiomyocytes cell line T0445.

Protein accession number	Description	Abundance ratio	Coverage (%)	Score Sequest HT	Peptide sequence	X corr (Top Charge)
P22626	heterogeneous nuclear ribonucleoproteins A2/B1	100	13	14.98	3	5.26
Q9Y490	Talin-1	100	3.5	21.79	5	6.07
P68363	Tubulin alpha-1B chain	10	18	27.75	6	5.81
P61981	14-3-3 protein gamma	8.8	20	33.69	3	5.28
P21333	Filamin-A	7.8	3.6	24.33	7	4.87
P62258-1	14-3-3 protein epsilon	6.7	15	20.09	3	6.3
Q04917	14-3-3 protein eta	6.4	20	19.44	4	4.55
P27348	14-3-3 protein theta	6.4	19	32.65	4	6.1
P31946	14-3-3 protein beta	5.7	21	46.44	3	6.49
P18206	Vinculin	5.4	6.4	37.04	7	6.34
P61978-2	Isoform 2 of Heterogeneous nuclear ribonucleoprotein K	4.4	6.8	14.37	3	4.32
P37802-2	Isoform 2 of Transgelin-2	4.2	29	43.48	5	6.73
P63104	14-3-3 protein zeta/delta	3.9	26	44.52	4	5.38
P55072	Transitional endoplasmic reticulum ATPase	3.9	15	50.47	8	5.69
P00338-3	Isoform 3 of L-lactate dehydrogenase A chain	3.7	7.9	18.76	3	4.96
P29401-2	Isoform 2 of Transketolase	3.6	7.5	18.19	2	6.32
P16104	Histone H2AX	3.1	48	48.9	4	6.07
P0DMV8	heat shock 70 kDa protein 1A	3	10	26.61	5	3.68
Q01995	transgelin	3	21	16	5	4.55
Q92688	Acidic leucine-rich nuclear phosphoprotein 32 family member B	2.9	19	16.16	2	5.42
Q12841	Follistatin-related protein 1	2.8	8	14.37	2	4.88
Q02818	Nucleobindin-1	2.8	6	20.54	2	4.06
P11142-1	Heat shock cognate 71 kDa protein	2.5	17	47.21	12	5.24
P15311	Ezrin	2.5	8.1	30.22	5	5.32
P04406	glyceraldehyde-3-phosphate dehydrogenase	2.3	21	35.04	6	4.84
P18669	Phosphoglycerate mutase 1	2.2	15	16.15	3	4.95
P08670	Vimentin	2.1	26	76.86	14	5.14

P07737	profilin-1	2	32	46.91	4	4.58
P26038	Moesin	1.9	8.4	30.15	6	5.46
P14618	Pyruvate kinase PKM	1.8	32	85.36	12	6
P60709	Actin, cytoplasmic 1	1.7	31	55.7	8	5.68
P06733-1	alpha-enolase	1.4	48	144	11	6.13

Supplementary Table 2. Proteomic profiling by nanoLC-MS/MS. 17 proteins were downregulated in both treated (ET-1 and Ang II) cardiomyocytes cell line T0445.

Accession	Description	Abundance ratio	Coverage [%]	Score Sequest HT	Peptides	X corr (Top Charge)
P19823	Inter-alpha-trypsin inhibitor heavy chain H2	0.492	5	20.53	4	6.19
P16402	Histone H1.3	0.439	15	24.97	4	5.55
P02774-3	Isoform 3 of Vitamin D-binding protein	0.383	8	20.56	2	5.85
P68104	Elongation factor 1-alpha 1	0.357	21	27.7	5	6.23
P01023	alpha-2-macroglobulin	0.186	2	35.51	3	4.74
P06396	Gelsolin	0.183	4	8.98	2	3.44
P09341	Growth-regulated alpha protein	0.114	27	19.9	2	6.30
P50990	T-complex protein 1 subunit theta	0.1	5	6.48	2	3.36
P48444	Coatomer subunit delta	0.1	5	5.89	2	3.58
O43707	Alpha-actinin-4	0.1	10	55.51	7	5.17
P78371-1	T-complex protein 1 subunit beta	0.01	6	9.48	2	5.23
P48643	T-complex protein 1 subunit epsilon	0.01	9	8.44	2	4.64
P16401	Histone H1.5	0.01	15	16.84	3	5.36
P13010	X-ray repair cross-complementing protein 5	0.01	3	5.05	2	3.81
P09211	Glutathione S-transferase P	0.01	19	9.6	2	5.73
P02765	Alpha-2-HS-glycoprotein	0.01	5	6.72	2	4.29
O75369-8	Isoform 8 of Filamin-B	0.01	2	24.4	4	6.66

Supplementary Table 3. Peptide sequences for quantitative analysis of 14-3-3 proteins

Protein accession number	Description	Peptide sequence	m/z	Fragment ion
P31946	14-3-3 beta	MTMDKSELVQKAKLAEQAERYDDMAAAMKAVTEQG HELSNEERNLLSVAYKNVVGARRSSWRVISSIEQKTERN EKKQQMGKEYREKIEAELQDICNDVLELLDKYLIPNAT QPESKVFYLKMKGDYFRYLSEVASGDNKQTTVSNSQQ AYQEAFEISKKEMQPTHPIRLGLALNFSVFYYEILNSPEK ACSLAK**TAFDEAIAELDTLNEESYK**DSTLIMQLLRDNL TLWTSENQGDEGDAGEGEN	720.7	769.3
P27348	14-3-3 theta	MEKTELIQKAKLAEQAERYDDMATCMKAVTEQGAELS NEERNLLSVAYKNVVGGRRSAWRVISSIEQKTDTSDKK LQLIKDYREKVESELR**SICTTVLELLDK**YLIANATNPES KVFYLKMKGDYFRYLAEVACGDDRKQTIDNSQGAYQE AFDISKKEMQPTHPIRLGLALNFSVFYYEILNNPELACTL AKTAFDEAIAELDTLNEDSYKDSTLIMQLLRDNLTLWTS DSAGEECDAAEGAEN	696.4	596.5
P63104	14-3-3 zeta/delta	MDKNELVQKAKLAEQAERYDDMAACMKSVTEQGAEL SNEERNLLSVAYKNVVGARRSSWRVVSSIEQKTEGAEK KQQMAREYREKIETELR**DICNDVLSLLEK**FLIPNASQAE SKVFYLKMKGDYYRYLAEVAAGDDKKGIVDQSQQAY QEAFEISKKEMQPTHPIRLGLALNFSVFYYEILNSPEKAC SLAKTAFDEAIAELDTLSEESYKDSTLIMQLLRDNLTLW TSDTQGDEAEAGEGGEN	710	596
P61981	14-3-3 gamma	MVDREQLVQKARLAEQAERYDDMAAAMKNVTELNEP LSNEERNLLSVAYKNVVGARRSSWRVISSIEQKTSADGN EKKIEMVRAYREKIEKELEAVCQDVLSLLDNYLIKNCSE TQYESKVFYLKMKGDYYRYLAEVATGEKRATVVESSE KAYSEAHEISKEHMQPTHPIRLGLALNYSVFYYEIQNAP EQACHLAK**TAFDDAIAELDTLNEDSYK**DSTLIMQLLRD NLTLWTSDQQDDDGGEGNN	711	755
P62258-1	14-3-3 epsilon	MDDREDLVYQAKLAEQAERYDEMVESMKKVAGMDV ELTVEERNLLSVAYKNVIGARRASWRIISSIEQKEENKG GEDKLKMIREYRQMVETELK**LICCDILDVLDK**HLIPAA NTGESKVFYYKMKGDYHRYLAEFATGNDRKEAAENSL VDIAYKAASDIAMTELPPTHPIRLGLALNFSVFYYEILNS PDRACRLAKAAFDDAIAELDTLSEESYKDSTLIMQLLRD NLTLWTSDMQGDGE EQNKEALQDVEDENQ	739	626
Q04917	14-3-3 eta	MGDREQLLQRARLAEQAERYDDMASAMKAVTELNEPL SNEDRNLLSVAYKNVVGARRSSWRVISSIEQKTMADGN EKKLEKVKAYREKIEK**ELETVCNDVLSLLDK**FLIKNCN DFQYESKVFYLKMKGDYYRYLAEVASGEKKNSVVEAS EAAYKEAFEISKEQMQPTHPIRLGLALNFSVFYYEIQNA PEQACLLAKQAFDDAIAELDTLNEDSYKDSTLIMQLLRD NLTLWTSDQQDEEAGEGN	874	1176.5

Supplementary Table 4. UHPLC-LTQ-Orbitrap Verlos Pro system: Gradient condition

Time (min)	Mobile A% 0.1% formic acid in H_20	Mobile B% 0.1% formic acid in ACN	Flow rate (mL/min)
0	100	0	0.25
15	40	60	0.25
17	0	100	0.25
20	0	100	0.25
21	100	0	0.25
40	100	0	0.25

Peptide standard	Product ion m/z	Fragment ion	Collision energy	Retention time (min)	LOD	LOQ	Range	Linearity
14-3-3 Zeta DICNDVLSLLEK	710	595 1030 1190	35	23.24	22.6 ng/mL	68 ng/mL	15 – 125 ng	0.995